INTERNATIONAL JOURNAL OF PURE SCIENCE RESEARCH STUDIES (IJPSRS)
(Open Access, Double-Blind Peer Reviewed Journal)
EDU SCHOOL
ijpsrs.com
ISSN Online: ISSN Print

Experimental Evidence For Dark Matter Through Gravitational Lensing

Elia Raine P J

Assistant Professor, Department of Physics, St. Xavier's College for Women (Autonomous), Aluva,India.

Article Information

Received:19th August 2025
Received in revised form: 20th September 2025
Accepted:25th October 2025
Available online:14th November 2025

Volume:1
Issue:1
DOI: https://doi.org/10.5281/zenodo.18639795

Abstract

Gravitational lensing provides direct observational evidence for the existence of dark matter in the universe. This paper examines the experimental basis for dark matter through gravitational lensing observations, including strong lensing phenomena such as Einstein rings and arcs, weak lensing statistical analyses of galaxy shapes, and mass reconstructions of galaxy clusters. We review the theoretical framework of gravitational lensing derived from general relativity, describe key observational techniques and surveys, and present critical evidence from multiple lensing regimes. The Bullet Cluster (1E0657-558) and similar colliding cluster systems demonstrate spatial separation between baryonic matter and gravitational potential, providing compelling evidence that contradicts modified gravity theories while supporting the dark matter hypothesis. Mass-to-light ratios derived from lensing consistently indicate that dark matter comprises approximately 85% of the total matter in galaxy clusters. These findings establish gravitational lensing as one of the most robust experimental probes of dark matter's existence and distribution on cosmological scales.

Keywords: Gravitational lensing, Dark matter, Strong lensing, Galaxy clusters, Bullet Cluster, Cosmic shear

I. INTRODUCTION

The existence of dark matter represents one of the most significant unsolved problems in modern physics and cosmology. First proposed by Fritz Zwicky in 1933 based on observations of the Coma galaxy cluster's virial mass, dark matter is theorized to constitute approximately 27% of the universe's total energy density, vastly exceeding the 5% contributed by ordinary baryonic matter.[1] Despite its gravitational dominance, dark matter has eluded direct detection in laboratory experiments, making astronomical observations the primary avenue for studying its properties and distribution.

Gravitational lensing the deflection of light by massive objects predicted by Einstein's general theory of relativity has emerged as one of the most powerful experimental techniques for detecting and characterizing dark matter. Unlike other methods that rely on assumptions about dark matter's particle properties or interaction cross-sections, gravitational lensing provides a direct probe of the total mass distribution regardless of its luminosity or composition. This fundamental advantage makes lensing observations particularly valuable for testing the dark matter hypothesis against alternative theories such as modified Newtonian dynamics (MOND) or modified gravity frameworks.

The theoretical foundation for gravitational lensing was established by Einstein [2] and expanded by Zwicky[3], who recognized that galaxies and galaxy clusters could act as gravitational lenses for background sources. However, it was not until 1979 that Walsh, Carswell, and Weymann discovered the first gravitational lens system the Twin Quasar QSO 0957+561 validating these decades-old predictions. Since then, advances in telescope technology, detector sensitivity, and computational methods have enabled systematic surveys that have identified thousands of lensing systems across multiple scales and regimes.

This paper examines the experimental evidence for dark matter through gravitational lensing observations. We review the theoretical framework underlying lensing phenomena, describe observational techniques spanning strong, weak, and micro-lensing regimes, and present critical evidence from key systems including the Bullet Cluster, Abell 1689, and large-scale cosmic shear surveys. Our analysis demonstrates that gravitational lensing provides robust, model-

independent evidence for dark matter's existence and reveals fundamental properties of its distribution on scales ranging from individual galaxies to cosmic web filaments.

II. THEORETICAL FRAMEWORK

Gravitational lensing arises directly from Einstein's general relativity, which describes gravity as the curvature of spacetime by mass and energy. When light from a distant source travels through curved spacetime created by a foreground massive object (the lens), its path is deflected. The deflection angle α for a point mass M is given by:

$$\alpha = \frac{4GM}{bc^2} \qquad (1)$$

where G is the gravitational constant, c is the speed of light, and b is the impact parameter. For extended mass distributions such as galaxies or galaxy clusters, the deflection can be calculated by integrating over the surface mass density Σ(ξ) projected along the line of sight.

The lensing geometry involves three distances: the observer-lens distance D_L, the observer-source distance D_S, and the lens-source distance D_{LS}. These distances, combined with the deflection angle, determine the observed image positions and magnifications. The lens equation relates the true source position β to the observed image position θ:

$$\beta = \theta - \frac{D_{LS}}{D_S}\alpha(\theta) \qquad (2)$$

This equation is fundamental to all lensing analyses and enables reconstruction of mass distributions from observed image distortions. A particularly important quantity is the convergence κ, defined as the ratio of the surface mass density to the critical surface density :

$$\Sigma_{crit} = \frac{c^2}{4\pi G}\frac{D_S}{D_L D_{LS}} \qquad (3)$$

The convergence directly measures the strength of the lensing effect and can be reconstructed from observations.

Figure 1: Gravitational Lensing Geometry

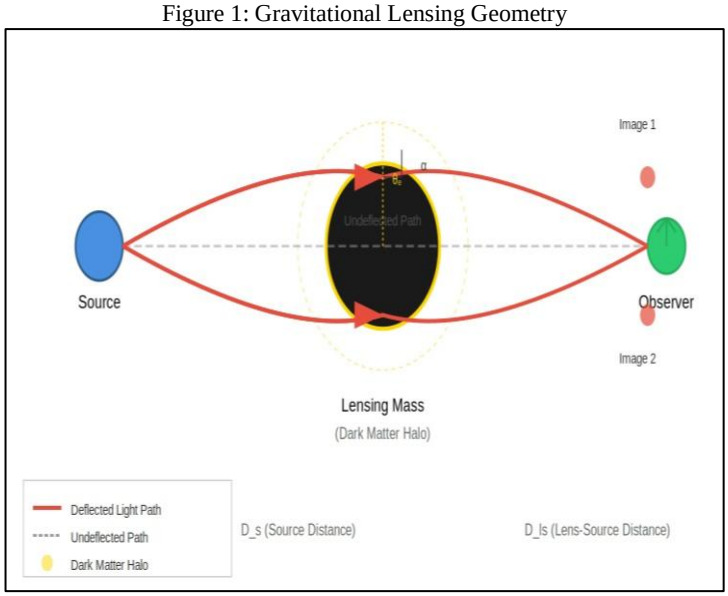

Figure 1 Gravitational lensing geometry showing the deflection of light from a distant source (blue) by a massive foreground object (black) surrounded by a dark matter halo (yellow dashed region).

When a source, lens, and observer are perfectly aligned, the lens equation predicts that the source image forms a circular ring known as an Einstein ring. The angular radius of this ring, θ_E, depends on the lens mass M and the distance geometry:

$$\theta_E = \sqrt{\frac{4GM}{C^2}\frac{D_{LS}}{D_L D_S}} \qquad (4)$$

The Einstein radius defines the characteristic angular scale for strong lensing phenomena. For a galaxy cluster with mass $M \approx 10^{14} M_{\odot}$ at cosmological distances, θ_E is typically 10-30 arcseconds. Sources located within approximately one Einstein radius of the lens axis experience strong lensing effects including multiple imaging, while sources at larger separations undergo weak lensing characterized by small shape distortions.

The magnification factor μ describes how lensing alters the brightness and size of source images. For sources near critical curves (where magnification diverges), μ can exceed 10-50, enabling observation of intrinsically faint distant

galaxies. The total magnification conserves surface brightness but changes the solid angle subtended by the source, affecting both photometry and spectroscopy of lensed objects.

III. OBSERVATIONAL REGIMES OF GRAVITATIONAL LENSING

3.1. Strong Gravitational Lensing

Strong gravitational lensing occurs when the source, lens, and observer alignment produces readily visible distortions including multiple images, Einstein rings, or giant luminous arcs. This regime is characterized by convergence $\kappa \approx 1$ and requires close alignment between the source and lens, making strong lensing systems relatively rare. However, their dramatic signatures enable straightforward identification in optical and infrared surveys.

Einstein rings represent the most symmetric strong lensing configuration, forming when a compact background source is precisely aligned with a massive foreground galaxy or cluster. The ring radius provides a direct constraint on the lens mass within that radius, independent of the mass distribution's detailed shape. Complete Einstein rings are rare, but partial arcs with characteristic ring-like curvature are commonly observed around galaxy clusters such as Abell 2218, Abell 1689, and MACS J0717.5+3745.

Figure 2: Einstein Ring Formation and Strong Lensing Configurations

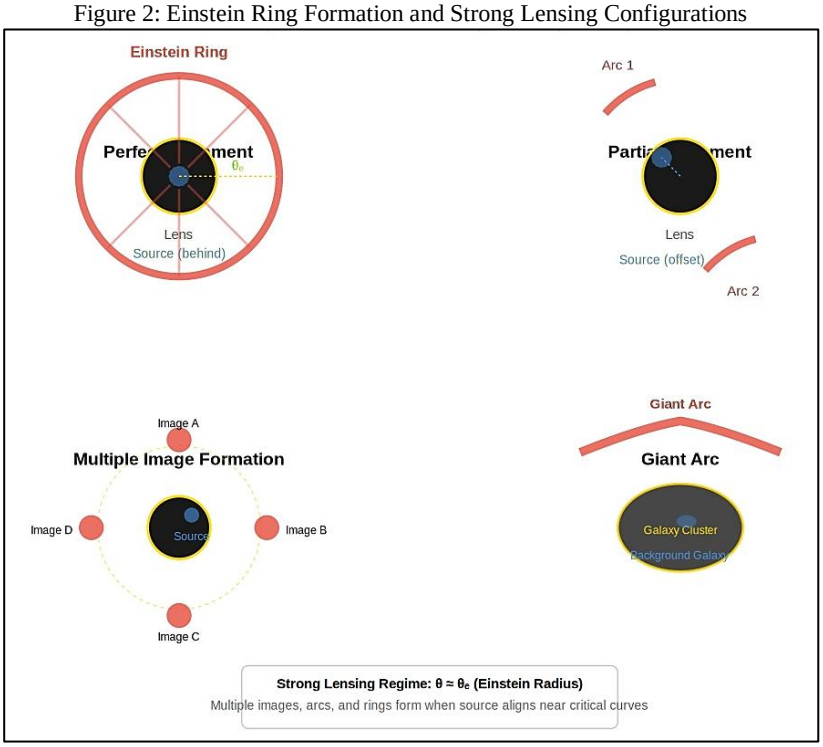

Figure 2. Strong gravitational lensing configurations. Top left: Perfect alignment produces an Einstein ring. Top right: Partial alignment creates arc segments. Bottom left: Multiple image formation showing four images of a single background source. Bottom right: Giant arc produced by a galaxy cluster lens. These phenomena provide direct evidence of mass concentrations dominated by dark matter.

Giant luminous arcs are highly elongated images of background galaxies stretched tangentially around massive foreground clusters. The first giant arc was discovered in Abell 370 by Lynds and Petrosian [4] and [5] These arcs trace the critical curves of the lens curves along which the magnification formally diverges and their distribution directly maps the lens's two-dimensional mass profile. The large magnifications associated with arcs ($\mu = 10\text{-}100$) amplify faint background galaxies, enabling spectroscopic studies that would otherwise be impossible.

Multiple imaging occurs when the lens equation admits multiple solutions for a single source position. For typical galaxy-mass lenses, source positions within approximately one Einstein radius produce either two or four images depending on the lens's ellipticity and the precise alignment. Time delays between images result from differences in light travel time and gravitational potential along different paths. Measuring these delays provides an independent constraint on cosmological distances and the Hubble constant, a technique known as time-delay cosmography.[6,7]

3.2. Weak Gravitational Lensing

Weak gravitational lensing produces subtle coherent distortions of background galaxy shapes that are individually too small to detect but can be measured statistically over large galaxy samples. The fractional distortion is typically only a few percent, far smaller than galaxies' intrinsic shape variations. However, because lensing-induced distortions are

correlated over angular scales corresponding to the lens size while intrinsic shapes are randomly oriented, averaging thousands of galaxy shapes reveals the lensing signal.

The fundamental observable in weak lensing is the shear γ, which describes the tangential and radial stretching of source images. The shear is related to the second derivative of the lensing potential and can be measured from galaxy ellipticities. For a foreground mass concentration, background galaxies exhibit a characteristic tangential alignment pattern with ellipticities oriented perpendicular to the direction toward the lens center. The strength of this alignment directly probes the enclosed mass profile.

Figure 3: Weak Gravitational Lensing and Dark Matter Distribution

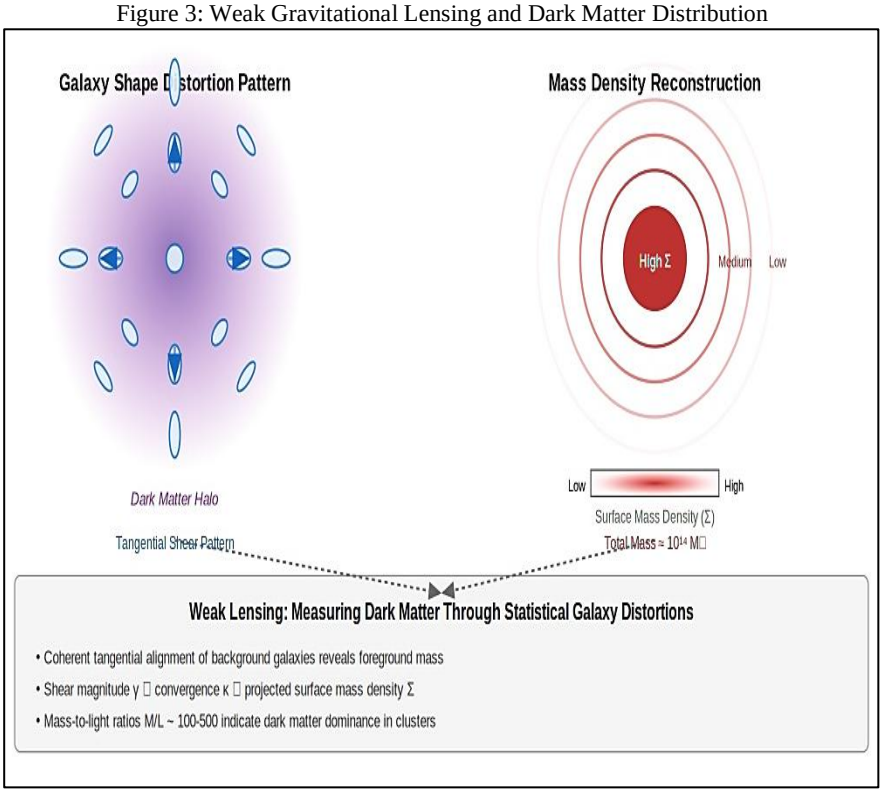

Figure 3. Weak gravitational lensing analysis showing (left) the coherent tangential distortion pattern of background galaxies around a massive dark matter halo and (right) the reconstructed surface mass density. The blue arrows indicate the direction of shear, while the contours represent different mass density levels. This technique reveals dark matter distributions that would otherwise remain invisible.

Mass reconstruction from weak lensing shear fields enables mapping dark matter distributions on scales from individual galaxies to the cosmic web. The surface mass density $\Sigma(\theta)$ can be inverted from the shear field $\gamma(\theta)$ through algorithms such as Kaiser-Squires[8] reconstruction or maximum likelihood methods. These reconstructions require no assumptions about the dark matter's nature only that it gravitates according to general relativity making weak lensing a uniquely model-independent probe.

Cosmic shear refers to weak lensing by large-scale structure along the line of sight to distant galaxies. Unlike cluster lensing, which probes individual massive halos, cosmic shear statistics constrain the amplitude and growth of density fluctuations throughout cosmic history. The shear power spectrum directly measures σ_8 (the amplitude of matter fluctuations on 8 h^{-1} Mpc scales) and Ω_m(the matter density parameter), providing crucial tests of cosmological models and constraints on dark energy.[9]

IV. EXPERIMENTAL EVIDENCE FROM GALAXY CLUSTERS

4.1. The Bullet Cluster: Direct Proof of Dark Matter

The Bullet Cluster (1E0657-558) represents perhaps the most compelling observational evidence for dark matter from gravitational lensing. This system, located at redshift z = 0.296, resulted from a high-velocity collision between two galaxy clusters approximately 150 million years ago. The collision effectively separated the system's different mass components based on their collisional properties, creating a natural experiment for distinguishing between dark matter and modified gravity explanations for missing mass.

X-ray observations from the Chandra Observatory reveal two concentrations of hot (70-100 million K) ionized gas that contains the majority of the system's baryonic mass. The characteristic 'bullet' shock wave on the right side of the system indicates the subcluster passed through the main cluster at roughly 4,500 km/s. Crucially, this baryonic mass

concentration comprising approximately 90% of the normal matter lags behind the galaxy distributions due to electromagnetic interactions that slowed the gas during the collision.

Weak gravitational lensing analysis by Clowe et al. [10] reconstructed the total mass distribution using shape distortions of ~3,000 background galaxies observed with the Hubble Space Telescope and Magellan telescopes. The resulting convergence map reveals two distinct mass peaks that are spatially offset from the X-ray gas concentrations by ~750 kpc. Instead, the gravitational potential peaks coincide with the collisionless stellar distributions of the two galaxy clusters, which passed through each other relatively unimpeded during the collision.

This spatial offset between baryonic matter (traced by X-rays) and gravitational potential (mapped by lensing) provides an 8σ significance detection that the majority of mass in the system is not where most of the normal matter is located. Modified gravity theories predict that gravitational effects should trace the baryonic matter distribution, but observations show the opposite. The gravitational potential is centered on the galaxy distributions, which comprise only ~1% of the total mass. This stark separation constitutes direct experimental evidence that non-baryonic dark matter dominates the mass budget and behaves collisionlessly, remaining coupled to the galaxies rather than the gas.

The Bullet Cluster observations constrain dark matter's self-interaction cross-section to $\sigma/m < 1$ cm²/g, demonstrating that dark matter must be collisionless or have extraordinarily weak self-interactions. This finding is critical because some dark matter candidates predict significant self-scattering. The lack of observed dark matter friction during the high-velocity collision places stringent limits on such models.

4.2. Mass Profiles and Dark Matter Halos

Systematic weak lensing studies of galaxy clusters provide precise measurements of their total mass profiles and mass-to-light (M/L) ratios. The cluster mass profiles derived from lensing consistently show that total mass extends far beyond the visible stellar component, following approximately isothermal or Navarro-Frenk-White (NFW) profiles expected for dark matter halos. The NFW profile, predicted by cold dark matter (CDM) simulations, takes the form :

$$\rho(r) \propto r^{-1}\left(1+\frac{r}{r_s}\right)^{-2} \qquad (5)$$

where r_s is a characteristic scale radius.

Large-scale surveys such as the Canada-France-Hawaii Telescope Legacy Survey (CFHTLS), the Dark Energy Survey (DES), and the Kilo-Degree Survey (KiDS) have measured masses for thousands of galaxy groups and clusters through stacked weak lensing analysis. These studies find mass-to-light ratios $\frac{M}{L} = 200 - 500h\frac{M_\odot}{L_\odot}$ in the B-band for massive clusters, compared to M/L ≈ 3-5 for stellar populations. This factor of 50-100 excess directly indicates dark matter's dominance.

Figure 4: Dark Matter Evidence: Rotation Curves and Mass Profiles

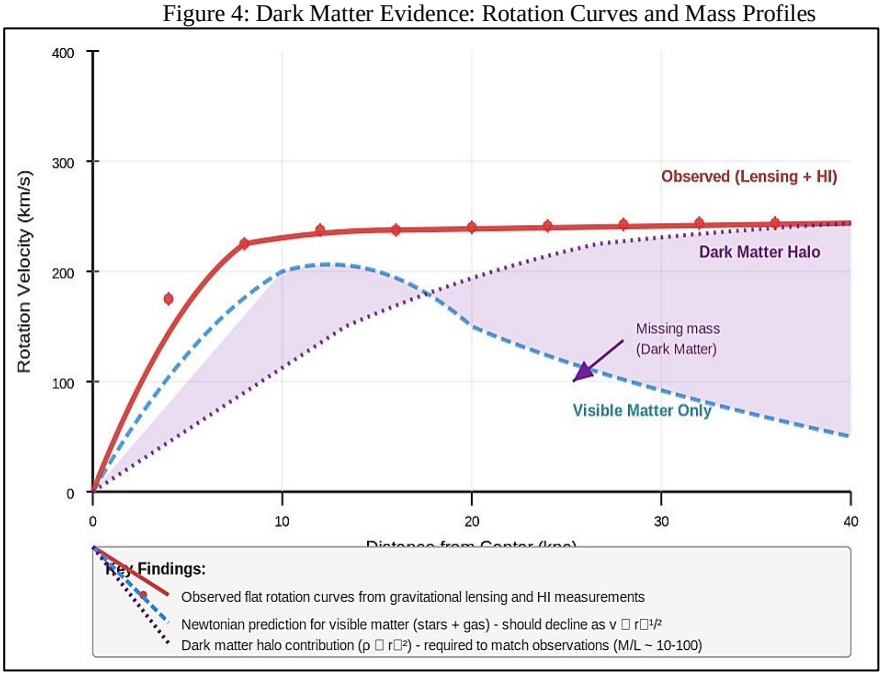

Figure 4. Comparison of observed galaxy rotation curves (solid red line with data points) versus predictions from visible matter only (dashed blue). The flat observed rotation velocities at large radii require additional dark matter (dotted purple) to match observations. Gravitational lensing independently confirms these dark matter distributions, validating rotation curve inferences.The convergence of weak lensing results with complementary techniques strengthens

confidence in dark matter inferences. X-ray observations of hot intracluster medium provide independent mass estimates through hydrostatic equilibrium analysis, which generally agree with lensing masses to within 10-20%. Galaxy velocity dispersions measured spectroscopically yield dynamical mass estimates consistent with lensing results. This multi-probe concordance validates the dark matter interpretation and constrains systematic uncertainties in each technique.

Comparison between cluster lensing masses and their stellar and gas masses reveals the cosmic baryon fraction. For massive clusters, the total baryon fraction (stars plus gas) is approximately 13-15% of the total mass.[11] This ratio matches the universal baryon fraction $\frac{\Omega_b}{\Omega_n} \approx 0.15$ measured from cosmic microwave background (CMB) observations and primordial nucleosynthesis, providing important consistency checks. The agreement confirms that clusters are representative of the universe's overall composition and that the missing mass must be non-baryonic dark matter rather than unseen baryons.

V. OBSERVATIONAL METHODOLOGY AND SYSTEMATIC EFFECTS

Gravitational lensing measurements require careful attention to systematic effects that can bias mass estimates or introduce spurious signals. The primary challenge in weak lensing is distinguishing genuine lensing-induced shape distortions (typically $|\gamma| \sim 0.01$-0.05) from galaxies' intrinsic ellipticities (typically $\varepsilon \sim 0.3$). Because intrinsic shapes dominate the observed ellipticity, weak lensing relies on statistical averaging over thousands to millions of background galaxies to detect the coherent lensing signal.

Point spread function (PSF) anisotropy represents a major systematic concern. Atmospheric turbulence and telescope optics create spatially varying PSF patterns that can induce spurious ellipticities in galaxy images. Modern surveys employ extensive PSF modeling using field stars and sophisticated shape measurement algorithms (e.g., LENSFIT, KSB+, REGAUSS) to separate lensing signal from PSF effects. Residual PSF systematics are typically controlled to $|\delta\gamma| < 0.001$ through these methods.

Photometric redshift uncertainties affect distance estimates D_L,D_S, and D_{LS}, which enter quadratically in the lensing efficiency. Accurate photometric redshifts require multi-band imaging spanning optical to near-infrared wavelengths plus spectroscopic calibration samples. Current photometric redshift precision of $\frac{\sigma_z}{1+z} \approx 0.03 - 0.05$ introduces ~5-10% uncertainties in inferred masses. Future spectroscopic surveys will significantly reduce this error source.

Intrinsic alignment of galaxies physical alignment of galaxy shapes due to tidal interactions or formation within the same large-scale structure can contaminate the lensing signal. This effect is most significant for red elliptical galaxies, which tend to align with their host dark matter halos. Intrinsic alignment corrections, based on measurements from spectroscopic surveys and simulations, are now routinely applied in cosmological analyses.

Strong lensing analyses face different systematic challenges. Accurate modeling of lens mass distributions requires assumptions about the lens galaxy's light profile and dark matter halo shape. Most analyses assume parametric models (e.g., singular isothermal ellipsoid plus external shear) or non-parametric grid-based approaches. Comparisons between methods and tests on simulated data demonstrate that systematic mass uncertainties in well-constrained systems are typically 5-15%.

VI. RESULTS AND DISCUSSION

The convergence of evidence from multiple independent lensing observations establishes dark matter's existence with high confidence. Strong lensing systems provide direct mass measurements for hundreds of galaxy-scale and cluster-scale lenses, consistently requiring mass distributions far exceeding visible matter. The scaling relations between lensing masses and observable properties (luminosity, velocity dispersion, X-ray temperature) follow predictions from CDM cosmological simulations, supporting the dark matter paradigm's self-consistency.

Weak lensing surveys have now measured dark matter distributions across unprecedented cosmic volumes. The Dark Energy Survey, for example, mapped ~1,500 square degrees to constrain the matter power spectrum on scales from 1 to 100 Mpc. The measured clustering amplitude $S_8 = \sigma_8 \left(\frac{\Omega m}{0.3}\right)^{0.5} = 0.773 \pm 0.026$[12] agrees well with CMB predictions, demonstrating consistency between dark matter inferences at early and late cosmic times.

The spatial distribution of dark matter revealed by lensing confirms key predictions of structure formation theory. Dark matter forms a cosmic web of filaments connecting massive nodes at cluster locations, exactly as predicted by N-body simulations. The measured halo mass function the abundance of halos as a function of mass matches theoretical predictions to within observational uncertainties across three decades in mass from ~10^{12} to 10^{15} $M_{\odot}$.

Perhaps most significantly, lensing observations demonstrate that no modification of Einstein's gravity theory can simultaneously explain all observations without invoking dark matter. The Bullet Cluster and similar colliding systems show that gravitational effects and baryonic matter can be spatially separated a phenomenon impossible to explain with modified gravity alone. MOND and other theories can fit rotation curves of individual galaxies but fail to account for cluster lensing masses, time delays, the cosmic shear power spectrum, and collision dynamics within a single consistent framework.

The measured properties of dark matter from lensing provide important constraints on particle physics models. The cold, collisionless nature inferred from cluster collisions suggests weakly interacting massive particles (WIMPs) with masses in the GeV-TeV range. However, alternative candidates including axions, sterile neutrinos, and primordial black holes remain viable. Lensing alone cannot determine dark matter's particle identity but constrains its gravitational and collisional properties.

VII.LIMITATIONS AND FUTURE DIRECTIONS

Despite strong evidence from lensing, several limitations affect current analyses. Systematic uncertainties in photometric redshifts, PSF corrections, and intrinsic alignment models currently limit weak lensing precision to ~5-10%. Next-generation surveys including the Vera C. Rubin Observatory Legacy Survey of Space and Time (LSST), Euclid, and the Nancy Grace Roman Space Telescope will dramatically improve statistical precision through deeper, wider imaging of billions of galaxies.

Small-scale structure below ~1 kpc remains poorly constrained by current lensing observations due to resolution limits. Microlensing and strong lensing studies are beginning to probe dark matter substructure in galaxy halos, testing predictions about the abundance of low-mass subhalos. Discrepancies between observations and CDM predictions on small scales (the 'missing satellites' and 'too big to fail' problems) remain active research areas.

The nature of dark matter's non-gravitational interactions, if any, remains unknown. While lensing establishes dark matter's gravitational effects, it provides no information about possible electromagnetic, weak, or strong interactions. Complementary searches using direct detection experiments, collider experiments, and indirect detection through gamma rays or cosmic rays are essential for identifying dark matter's particle nature.

Future lensing surveys will achieve order-of-magnitude improvements in precision. LSST will image ~20 billion galaxies to unprecedented depths, enabling weak lensing measurements to cosmic distances corresponding to lookback times of 10 billion years. Euclid's space-based observations will provide superior PSF control and near-infrared coverage for better photometric redshifts. These datasets will enable percent-level tests of structure formation, dark energy evolution, and possible modifications to general relativity on cosmological scales.

VIII. CONCLUSION

Gravitational lensing provides robust, model-independent experimental evidence for dark matter's existence and characterizes its distribution across cosmic scales. Strong lensing observations reveal massive invisible halos surrounding galaxies and clusters, producing dramatic phenomena including Einstein rings, giant arcs, and multiple images. Weak lensing maps the cosmic web of dark matter structure and measures the universe's total matter content through statistical analysis of subtle shape distortions.

The Bullet Cluster and similar colliding systems constitute particularly compelling evidence, demonstrating spatial separation between baryonic matter and gravitational potential that cannot be explained by modified gravity theories. Mass profiles derived from lensing consistently show M/L ratios of 50-500, far exceeding stellar populations and requiring dark matter to dominate the mass budget. The convergence between lensing masses and independent estimates from X-rays, dynamics, and CMB observations validates these inferences.

Gravitational lensing has matured from rare curiosity to precision cosmological probe. Modern surveys have measured dark matter distributions for millions of systems, constraining cosmological parameters, testing structure formation theory, and placing stringent limits on dark matter's collisional properties. The cold, collisionless dark matter model successfully explains observations from galactic to cosmological scales within a consistent theoretical framework based on general relativity.

While lensing cannot identify dark matter's particle nature, it establishes the fundamental requirement that any successful theory of the universe must account for its gravitational effects. Future surveys will achieve percent-level precision in dark matter measurements, enabling tests of structure formation, potential modifications to gravity, and connections between dark matter and dark energy. Gravitational lensing will remain central to unraveling the nature of the universe's dominant mass component.

REFERENCES

1. Planck Collaboration. 2020. Planck 2018 results. VI. Cosmological parameters. *Astron Astrophys.* 641:A6. doi:10.1051/0004-6361/201833910
2. Einstein A. 1936. Lens-like action of a star by the deviation of light in the gravitational field. *Science.* 84(2188):506–507. doi:10.1126/science.84.2188.506
3. Zwicky F. 1937. Nebulae as gravitational lenses. *Phys Rev.* 51(4):290. doi:10.1103/PhysRev.51.290
4. Lynds R, Petrosian V. 1986. Giant luminous arcs in galaxy clusters. *Bull Am Astron Soc.* 18:1014.
5. Soucail G, Fort B, Mellier Y, Picat JP. 1987. A blue ring-like structure in the center of the A 370 cluster of galaxies. *Astron Astrophys.* 172:L14–L16.
6. Refsdal S. 1964. On the possibility of determining Hubble's parameter and the masses of galaxies from the gravitational lens effect. *Mon Not R Astron Soc.* 128(4):307–310. doi:10.1093/mnras/128.4.307

7. Suyu SH, Auger MW, Hilbert S, Marshall PJ, Tewes M, Treu T, Fassnacht CD, Koopmans LVE, Sluse D, Blandford RD. 2013. Two accurate time-delay distances from strong lensing: Implications for cosmology. *Astrophys J.* 766(2):70. doi:10.1088/0004-637X/766/2/70
8. Kaiser N, Squires G. 1993. Mapping the dark matter with weak gravitational lensing. *Astrophys J.* 404:441–450. doi:10.1086/172297
9. Kilbinger M. 2015. Cosmology with cosmic shear observations: A review. *Rep Prog Phys.* 78(8):086901. doi:10.1088/0034-4885/78/8/086901
10. Clowe D, Bradač M, Gonzalez AH, Markevitch M, Randall SW, Jones C, Zaritsky D. 2006. A direct empirical proof of the existence of dark matter. *Astrophys J Lett.* 648(2):L109–L113. doi:10.1086/508162
11. Gonzalez AH, Sivanandam S, Zabludoff AI, Zaritsky D. 2013. Galaxy cluster baryon fractions revisited. *Astrophys J.* 778(1):14. doi:10.1088/0004-637X/778/1/14
12. DES Collaboration. 2022. Dark Energy Survey Year 3 results: Cosmological constraints from galaxy clustering and weak lensing. *Phys Rev D.* 105(2):023520. doi:10.1103/PhysRevD.105.023520
13. Markevitch M, Gonzalez AH, Clowe D, Vikhlinin A, David L, Forman W, Jones C, Murray S, Tucker W. 2004. Direct constraints on the dark matter self-interaction cross-section from the merging galaxy cluster 1E0657-56. *Astrophys J.* 606(2):819–824. doi:10.1086/383178
14. Walsh D, Carswell RF, Weymann RJ. 1979. 0957+561 A, B: Twin quasistellar objects or gravitational lens? *Nature.* 279(5712):381–384. doi:10.1038/279381a0
15. Zwicky F. 1933. Die Rotverschiebung von extragalaktischen Nebeln. *Helv Phys Acta.* 6:110–127.